Enhancement of $GABA_A$-current run-down in the hippocampus occurs at the first spontaneous seizure in a model of temporal lobe epilepsy

Manuela Mazzuferi[a,b,1], Eleonora Palma[c,d,1,2], Katiuscia Martinello[e], Francesca Maiolino[d], Cristina Roseti[c], Sergio Fucile[c,e], Paolo F. Fabene[f], Federica Schio[f], Michele Pellitteri[f], Guenther Sperk[g], Ricardo Miledi[h,i,2], Fabrizio Eusebi[c,e,3], and Michele Simonato[a,b,2]

[a]Department of Clinical and Experimental Medicine, Section of Pharmacology, and Neuroscience Center, and [b]National Institute of Neuroscience, University of Ferrara, 44100 Ferrara, Italy; [c]Istituto Pasteur-Fondazione Cenci Bolognetti and Dipartimento di Fisiologia e Farmacologia-Centro di Eccellenza Biologia e Medicina Molecolare, Università di Roma "La Sapienza", 00185 Rome, Italy; [d]San Raffaele Pisana Istituto di Ricovero e Cura a Carattere Scientifico, IRCCS, 00166 Rome, Italy; [e]Neuromed Istituto di Ricovero e Cura a Carattere Scientifico, 86077 Pozzilli, Isernia, Italy; [f]Department of Morphological and Biomedical Sciences, Section of Anatomy, University of Verona, 37134 Verona, Italy; [g]Department of Pharmacology, Medical University, 6020 Innsbruck, Austria; [h]Instituto de Neurobiología, AP1-1141Querétaro, Mexico; and [i]Department of Neurobiology and Behavior, University of California, Irvine, CA 92697-4550

Contributed by Ricardo Miledi, December 27, 2009 (sent for review November 25, 2009)

Refractory temporal lobe epilepsy (TLE) is associated with a dysfunction of inhibitory signaling mediated by $GABA_A$ receptors. In particular, the use-dependent decrease (run-down) of the currents (I_{GABA}) evoked by the repetitive activation of $GABA_A$ receptors is markedly enhanced in hippocampal and cortical neurons of TLE patients. Understanding the role of I_{GABA} run-down in the disease, and its mechanisms, may allow development of medical alternatives to surgical resection, but such mechanistic insights are difficult to pursue in surgical human tissue. Therefore, we have used an animal model (pilocarpine-treated rats) to identify when and where the increase in I_{GABA} run-down occurs in the natural history of epilepsy. We found: (*i*) that the increased run-down occurs in the hippocampus at the time of the first spontaneous seizure (i.e., when the diagnosis of epilepsy is made), and then extends to the neocortex and remains constant in the course of the disease; (*ii*) that the phenomenon is strictly correlated with the occurrence of spontaneous seizures, because it is not observed in animals that do not become epileptic. Furthermore, initial exploration of the molecular mechanism disclosed a relative increase in α4-, relative to α1-containing $GABA_A$ receptors, occurring at the same time when the increased run-down appears, suggesting that alterations in the molecular composition of the GABA receptors may be responsible for the occurrence of the increased run-down. These observations disclose research opportunities in the field of epileptogenesis that may lead to a better understanding of the mechanism whereby a previously normal tissue becomes epileptic.

$GABA_A$ receptor | pilocarpine rat | *Xenopus* oocytes

Epilepsies originating in the temporal lobe of the brain are the most common in adults. Focal pathological abnormalities can be observed in patients suffering these diseases, the most prominent of which is a loss of neurons in the hippocampus (hence termed hippocampal sclerosis). These abnormalities develop in a previously apparently healthy tissue, often after an initial "epileptogenic" event that can produce damage, for example, an episode of prolonged, uncontrolled seizures [status epilepticus, (SE)]. After a latent period of weeks to years, epileptogenic events may be followed by the occurrence of spontaneous recurrent seizures (SRS), i.e. epilepsy (1). Unfortunately, currently available antiseizure drugs do not prevent this process, and patients with medically intractable epilepsy may become seizure-free only after resective surgery.

Refractory temporal lobe epilepsy (TLE) has been shown to be associated with a dysfunction of the inhibitory signaling mediated by $GABA_A$ receptors (2–4). In particular, the repetitive activation of $GABA_A$ receptors produces a use-dependent decrease (run-down) of the membrane currents evoked by GABA (I_{GABA}), a phenomenon markedly enhanced in hippocampal and cortical neurons of TLE patients (5, 6). This phenomenon is significantly prevented by BDNF, adenosine derivatives, and phosphatase inhibitors (7–10), suggesting that phosphorylation of $GABA_A$ receptors and/or associated proteins may be linked to the increase in run-down (11). Understanding the role of I_{GABA} run-down in the disease and its mechanisms may allow development of medical alternatives to surgical resection.

However, analysis of human tissue precludes the possibility of understanding when, in the natural history of the disease, the enhancement of I_{GABA} run-down appears and, thus, to understand its role in the physiopathology of the disease. More recently, increased run-down has been found to be present, with identical characteristics, in rats made chronically epileptic with the use of pilocarpine (6). The pilocarpine model reproduces some of the key features of human TLE (1): an episode of SE produces intense neuronal damage [mainly by inflammatory mechanisms] (12, 13) and, after a latent period of approximately 2 weeks, SRSs (14). We decided to take advantage of this model for identifying precisely when and where the increase in I_{GABA} run-down occurs in the natural history of epilepsy by correlating key pathological (cell damage) and behavioral (SRSs) features of the disease progression with the I_{GABA} current run-down in the hippocampus and in the neocortex.

Results and Discussion

Natural History of Pilocarpine-Induced Epilepsy. Pilocarpine (300 mg/kg i.p.) rapidly induced a robust convulsive SE [latency: 19 ± 1 min, mean ± SEM, $n = 44$; ref. 14], which was interrupted after 3 h by administering the anticonvulsant diazepam (10 mg/kg i.p.). The development of epilepsy was then evaluated using video-EEG. Following interruption of SE, the animals continued to experience occasional, self-limiting generalized seizures (less than 1-min duration) for 2–3 days, before entering a latency state in which they were apparently well. The first spontaneous seizure occurred 9 ± 1 days after SE (mean ± SEM, $n = 28$). In rare

Author contributions: M.M., E.P., S.F., R.M., F.E., and M.S. designed research; M.M., E.P., K.M., F.M., C.R., S.F., P.F.F., F.S., M.P., and M.S. performed research; G.S. contributed new reagents/analytic tools; M.M., E.P., K.M., F.M., C.R., S.F., and M.S. analyzed data; and M. M., E.P., S.F., R.M., F.E., and M.S. wrote the paper

The authors declare no conflict of interest.

[1]M.M. and E.P. contributed equally to this work.

[2]To whom correspondence may be addressed. E-mail: michele.simonato@unife.it or eleonora.palma@uniroma1.it or rmiledi@uci.edu.

[3]Deceased October 26, 2009.

This article contains supporting information online at www.pnas.org/cgi/content/full/0914710107/DCSupplemental.

cases, some rats did not display any spontaneous seizure for the total length of the observation (2 months) and were therefore classified as "resistant" to epilepsy development. In contrast, all other animals kept experiencing SRSs with a mean frequency of 4 ± 2 seizures per day (mean ± SEM, $n = 16$; duration about 1 min each, severity class 4–5 plus running; ref. 15). Interestingly, these seizures tended to occur in clusters, as described by others (16, 17), i.e., days with frequent seizures alternating with days with few or no seizures.

For evaluation of the pathological correlates of these phenomena (cell damage in particular), animals were killed at different time-points after the epileptogenic insult (SE), representative of the different phases of the natural history of the disease (Fig. 1*A*): 24 h (acute phase immediately following the epileptogenic insult), 5 days (latency), 6 h after the first spontaneous seizure (beginning of the symptoms of epilepsy), 2 weeks after the first seizure (chronic epilepsy), 2 months after the first seizure ("late" chronic phase). Fluoro-Jade C (FJC), a staining procedure that allows identification of degenerating cells, demonstrated ongoing damage in several brain areas. In the neocortex, numerous FJC-positive cells began to appear in layers II and III already in the acute phase, but peak neurodegeneration was reached during the latency period (5 days after SE). Subsequently, this phenomenon gradually subsided, such that no sign of ongoing degeneration was observed 1 and 2 months after SE (Fig. 1*B*). A parallel development was observed in the hippocampus. Degenerating cells were observed in CA1, CA3, and in the hilus of the dentate gyrus, reminiscent of hippocampal sclerosis (18). As for the neocortex, this pattern of damage was clearly detectable at 24 h, peaked during latency and was already subsiding at the time of the first seizure, becoming undetectable 1 and 2 months after SE (Fig. 1 *B* and *C*). No sign of ongoing damage was detected in the resistant rat of this experimental group (Fig. 1 *B* and *C*), but this was not surprising because this animal was killed 2 months after SE, when no residual ongoing damage was observed even in chronically epileptic rats.

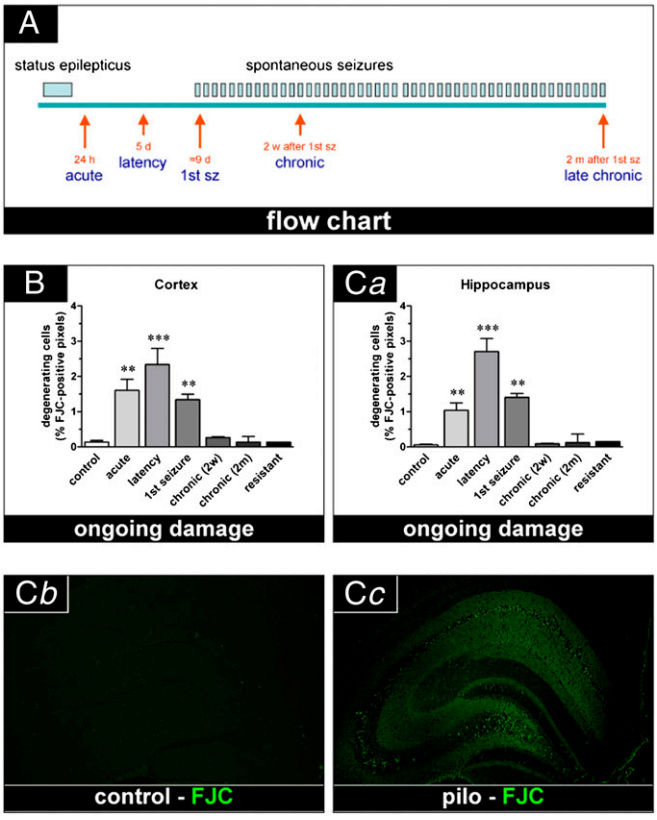

Fig. 1. (*A*) Schematic diagram of the in vivo experiments. The time points of analysis are indicated by red arrows. See text for details. (*B*) Time course of neurodegeneration in the neocortex. Shown is the percent of FJC-positive pixels (calculated as described in the *Materials and Methods*) in naïve controls and in pilocarpine-treated rats killed at different time-points in the course of the disease, as indicated. Data are the means ± SE of four to five animals per group. The black bar represents data from a resistant animal that did not display any spontaneous seizure in the 2 months of observation. $^{**}P < 0.01$, $^{***}P > 0.001$ vs. naïve; Kruskal-Wallis test. (*Ca*) Time course of neurodegeneration in the whole hippocampus. Data are the means ± SE of four to five animals per group, and are presented like in *A*. (*Cb*) and (*Cc*) Representative images of the effect of pilocarpine SE on degeneration in the hippocampus. Degenerating cells are marked with FJC (green). In a naïve control, no detectable FJC signal is observed (*Cb*); in contrast, 5 days after pilocarpine (pilo)-induced SE, hippocampal damage is detectable in many subareas, as described in the text.

As stated above, FJC provides an estimate of ongoing damage (cells undergoing degeneration at a specific time) but not of the resulting "cumulative" lesion (19). To obtain an estimate of cumulative damage, we performed further experiments to evaluate loss of neurons, astrocytosis, and volume of the hippocampus. First, we measured the relative representation of astrocytes and neurons in the hippocampus using GFAP and microtubule-associated protein-2 (MAP2) immunofluorescence: as expected, the SE-damaged hippocampus presents a clearly reduced density of neuronal cells, most notably hilar and pyramidal cells (Fig. S1). We then measured the density of astrocytes and neurons in the different phases of the disease using immunofluorescence. Neuronal density was measured using the marker NeuN. This parameter was already significantly decreased 24 h after SE, reached a minimum during latency (around day 5), and was still significantly reduced at 2 months (Fig. 2*A*). Immunofluorescence also allowed identification of the subareas in which this phenomenon occurred: dentate gyrus granule cells were not significantly decreased, whereas neurons in the CA1 and CA3 pyramidal layer, as well as interneurons in the dentate hilus and in the strata oriens and radiatum of CA1 and CA3, were greatly decreased in animals that experienced SE. In contrast, the density of GFAP-positive cells (putative astrocytes) in the entire hippocampus was significantly increased in the pilocarpine animals, compared with naïve controls, an indication of reactive astrocytosis (19, 20). This phenomenon developed with a time course reflecting the one described for neurons: it was already significant 24 h after SE, reached its maximum during latency (around day 5), but then gradually decreased, being virtually absent at 2 months (Fig. 2*B*). In terms of hippocampal volume, a 3D structural reconstruction demonstrated a 28 ± 3% reduction 3 days after pilocarpine administration, as compared with control animals ($P < 0.001$, Mann-Whitney *u* test for unpaired data); this 30% reduction in size was still present in chronic animals.

I_{GABA} Run-Down. We then asked when, in the natural history of the disease, the increased I_{GABA} run-down appeared. Accordingly, animals were killed at the time-points described above and membranes were prepared from the hippocampus and from the temporal cortex. To study the actual rat $GABA_A$ receptors, we first applied the "microtransplantation" method, which consists in injecting *Xenopus* oocytes with membranes from foreign tissues. The oocyte's plasma membrane incorporates the foreign membranes and efficiently acquires functional neurotransmitter receptors and channels. These proteins retain the properties that they have in their native tissues (21, 22) and are still embedded in their natural lipid membrane (23). In agreement with previous experiments (6), applications of GABA (1 mM) to oocytes injected with rat membranes elicited I_{GABA} of variable amplitudes (range: −300 nA to 10 nA) that exhibited a variable run-down after repetitive GABA applications (589 oocytes/31 frogs, 25 different rats). I_{GABA} run-down was not related to changes in I_{GABA} reversal potential, as proven in nine oocytes by using

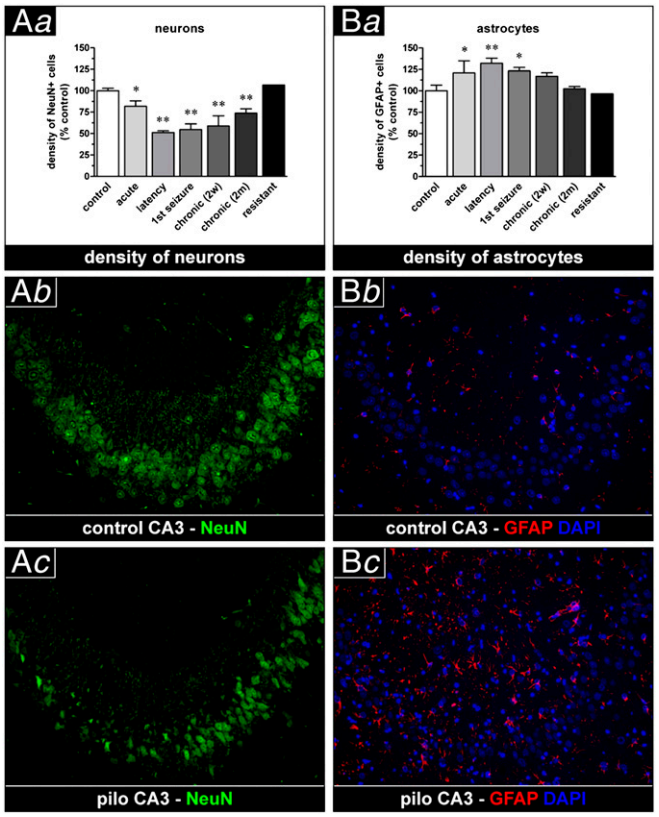

Fig. 2. Neuronal loss and astrocytosis at various time points after pilocarpine-induced SE. (*Aa*) Measure of the density of NeuN-positive neurons in the whole hippocampus of naïve controls and of pilocarpine-treated rats killed at different time-points in the course of the disease, as indicated. The black bar represents data from a resistant animal that did not display any spontaneous seizure in the 2 months of observation. The other data are the means ± SEM of four to five animals per group. $*P < 0.05$, $**P < 0.01$ vs. naïve; ANOVA and post hoc Newman-Keuls test. (*Ab*) and (*Ac*) Representative images showing NeuN-positive (green) cells in the CA3 area of a control (*Ab*) and of a pilocarpine (pilo) rat killed during latency, 5 days after SE (*Ac*). Note the loss of positive cells in the latter. (*Ba*) Measure of the density of GFAP-positive cells in the hippocampus. Data are represented as in *Aa* and are the means ± SEM of four to five animals per group. $*P < 0.05$, $**P < 0.01$ vs. naïve; ANOVA and post hoc Newman-Keuls test. (*Bb* and *Bc*) Representative images showing GFAP-positive (red) cells in the CA3 area of a control (*Bb*) and of a pilocarpine (pilo) rat killed during latency, 5 days after SE (*Bc*). Note the increase in the number of positive cells in the latter.

voltage ramps during the first vs. the sixth GABA application (one frog, two rats; −24 ± 0.39 mV vs. −23 ± 0.5 mV; $P > 0.1$). As compared with controls, I_{GABA} run-down was not modified in the acute phase (24 h after SE) nor during latency (Fig. 3 and Table S1). In contrast, oocytes injected with membranes isolated from the hippocampus of rats killed immediately after the first spontaneous seizure exhibited an obviously increased I_{GABA} run-down (control: fall to 68 ± 6%, mean ± SEM, range 51–88%, 32 oocytes/3 frogs); first seizure hippocampus: fall to 28 ± 6% (range 16–39%, 60/5, $P < 0.01$; Fig. 3 and Table S1). I_{GABA} run-down was not accompanied by a significant change in I_{GABA} decay ($T_{0.5}$ = 5.0 ± 0.5 s vs. $T_{0.5}$ = 5.3 ± 0.6 s in controls and first seizure hippocampi, respectively, 14/3, $P > 0.1$) nor between the first and sixth GABA application (5.2 ± 0.5 s vs. 4.8 ± 0.8 s, 12/2, $P > 0.1$). This increased run-down was then maintained throughout the course of the disease with almost identical characteristics for the entire period of observation (up to 2 months after the first spontaneous seizure; Fig. 3*A* and Table S1). Importantly, no alteration in I_{GABA} run-down was observed in "resistant" animals (60 ± 2%, 35/4, 3 rats) that did not display any SRS during the period of observation (Fig. 3*A* and Table S1). In contrast with the hippocampus, no significant change was observed in the cortex at the time of the first spontaneous seizure, but I_{GABA} run-down was found to increase in the chronic phase (35 ± 4%, 70/8 and 37 ± 42%, 30/3, 2 weeks and 2 months after the first spontaneous seizure, respectively, three rats in each group; Fig. 3*B* and Table S1). Again, no alteration was observed in "resistant" animals (64 ± 3%, 35/4, three rats; Fig. 3*B*).

These findings were verified in whole-cell patch clamped hippocampal pyramidal neurons in rat brain slices. Specifically, applications of GABA (100 μM) evoked whole-cell currents, with a maximal amplitude of 1.3 ± 0.2 nA (range 0.4–2.9 nA; n = 11) in controls of 1.2 ± 0.2 nA (range 0.3–1.8 nA; n = 6) in slices from rats in acute phase and of 1.7 ± 0.3 nA (range 0.6–2.9 nA; n = 9) in slices from rats in chronic phase. Repetitive GABA applications (1 s every 15 s) induced a significantly greater current run-down in neurons of the chronic group compared both with the control and acute groups (Fig. 4): GABA response decreased to 46 ± 4% in the chronic group (n = 9) vs. 62 ± 5% in the control (n = 11; $P < 0.05$) and 69 ± 3% in the acute group (n = 6; $P < 0.05$).

Molecular Mechanisms of I_{GABA} Run-Down. The molecular mechanisms underlying the changes are still unknown. However, it can be hypothesized that they depend on alterations in $GABA_A$ receptor subunit composition within specific cell populations. Indeed, changes in the expression levels (thus, in the expected molecular composition) of $GABA_A$ receptors have been described in several epilepsy models. One common trait that has been identified by many is an increased expression of the α4 subunit, although the α1 subunit has been reported to be slightly increased, unaltered, or even decreased (24–27). Taken together, these data indicate a shift in balance toward an increase in the relative representation of α4- compared with α1-containing $GABA_A$ receptors. This alteration has been hypothesized to be proepileptic because (1) epileptogenic insults (lithium-pilocarpine treatment) increase the α1 subunit expression in immature rats, which are less susceptible than adults to the development spontaneous seizures (28); (2) the α1 subunit is significantly more expressed in slow-kindling than in fast kindling rats (29); (3) viral vector-mediated correction of the alteration in the α1/α4 ratio inhibits epilepsy development in the pilocarpine model (30). Interestingly, a recent study (31) shows that α4-containing $GABA_A$ channels possess characteristics that imply a reduced GABA response to high frequency stimulation: reduced activation rate, prolonged desensitization, reduced response to repetitive GABA application (i.e., increased run-down). None of these studies, however, describes the evolution of these molecular changes with the natural history of the disease and their correlation with the appearance and maintenance of increased run-down. If a shift in balance toward an increase in the relative representation of α4- compared with α1-containing $GABA_A$ receptors is to play a role in $GABA_A$ receptor desensitization, then it should appear in the same site and at the same time in the natural history of experimental epilepsy when the increase in I_{GABA} current run-down appears, i.e., in the hippocampus at the time of the first spontaneous seizure.

To explore this possibility, we performed an immunohistochemistry and double-label immunofluorescence analysis of the representation of α1 and α4 $GABA_A$ subunits in the rat hippocampus and cortex, at the different stages of progression of the disease. In the hippocampus, as previously reported (32), we found that the α1 subunit is more expressed in parvalbumin-positive interneurons than in principal pyramidal or granular cells, although the α4 subunit is prominent in pyramidal cells (Fig. S2, *C* and *F*). A significant reduction in the density of α1 subunit and increase in α4 subunit density were observed at the time of the first seizure (Fig. S2, *A*, *B*, *D*, and *E*). Thus, the α1 to

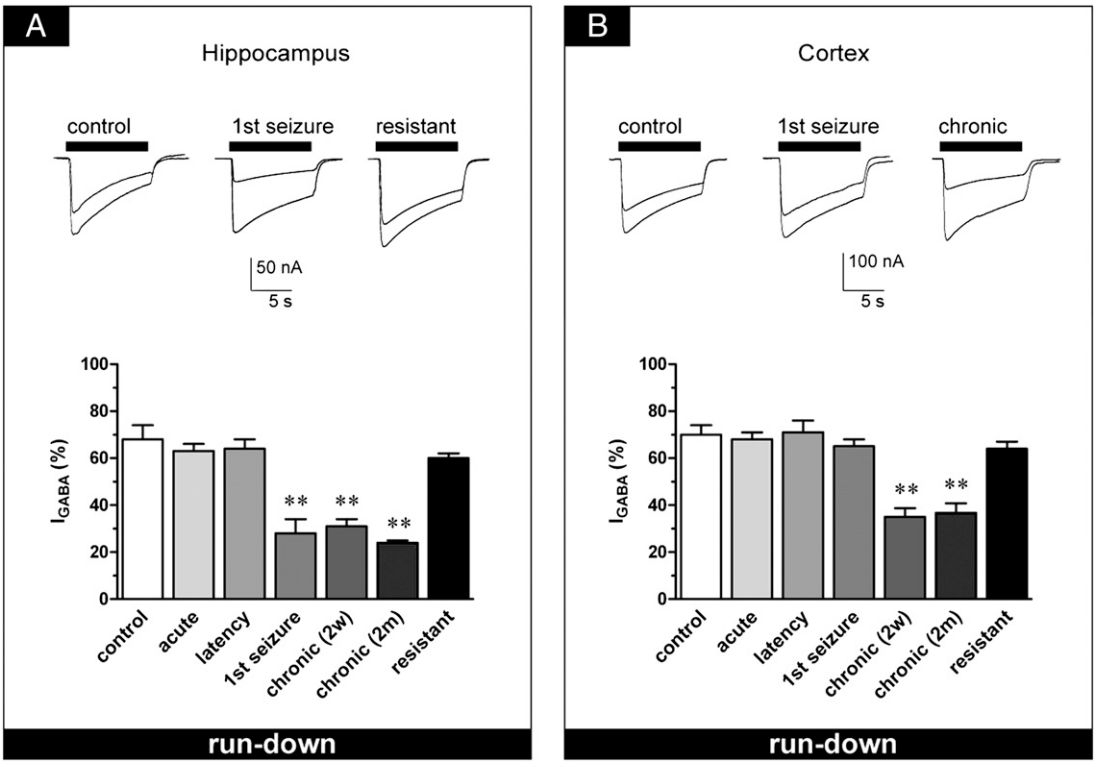

Fig. 3. I_{GABA} run-down from oocytes injected with membranes prepared from rats killed at various time points after pilocarpine-induced SE. (*A Upper*) Superimposed currents elicited by the first and sixth GABA (1 mM, 10-s duration every 40 s, horizontal bar) applications in oocytes injected with hippocampal rat membranes, as indicated. Samples from three different oocytes representative of 32 (*Left*), 60 (*Center*), and 35 (*Right*) experiments. Holding potential, −60 mV. Note the small I_{GABA} run-down in the resistant animal (2 months after SE). (*Lower*) I_{GABA} run-down in oocytes injected with hippocampal membranes. Data are the means ± SEM of 30–66 oocytes per group (three to five rats). I_{GABA} peak values were normalized to the first I_{GABA} peak current amplitude. GABA 1 mM, 10-s duration. $^{**}P < 0.01$ vs. control. ANOVA and post hoc Holm-Sidak test. (*B Upper*) superimposed currents elicited as in (*A*) in oocytes injected with cortical rat membranes. Samples from three oocytes representative of 56 (*Left*), 65 (*Center*), and 30 (*Right*) experiments. (*Lower*) I_{GABA} run-down in oocytes injected with cortical membranes. Data are the means ± SEM of 30–70 oocytes per group (three to eight rats). Normalization of I_{GABA}, GABA concentration and holding potential as in *A*. Note the small I_{GABA} run-down in the first seizure animals compared with *A*. $^{**}P < 0.01$ vs. control. ANOVA and post hoc Holm-Sidak test.

α4 ratio underwent a significant shift toward α4, and this new situation was maintained all along the chronic period, perfectly paralleling the increase in I_{GABA} run-down (Fig. 5). Coherently, no alteration in the α1 to α4 ratio was observed in the resistant animal of this group (Fig. 5). In the cortex, although no significant alteration was observed in the expression levels of the α1 subunits, we observed a twofold up-regulation in the α4 in the chronic period but not at the time of the first spontaneous seizure (that is, the increase in the α1 to α4 ratio paralleled the increase in GABA run-down also in the cortex).

Discussion and Conclusions

In summary, we found that the increased run-down of the $GABA_A$ current begins in the hippocampus at the time of the first spontaneous seizure. Because the $GABA_A$ current run-down may make the tissue hyper-excitable, it can be hypothesized that it represents a switch leading from latency to spontaneous seizures, i.e., epilepsy.

It can be hypothesized that this switch may be produced by an alteration in the receptor molecular composition. In the frame of this study, we tested this hypothesis focusing on changes in the α1 and α4 GABA receptor subunits. However, this may be just one among other possible molecular mechanisms, because substantial alterations in several other subunits have been reported in association with epilepsy. For example, expression of the δ-subunit has been reported to be consistently reduced in granule cell dendrites (25, 33, 34) and may be substituted by γ2-subunits, resulting in impairment of both tonic and phasic GABA transmission (35). Furthermore, verification at single cell level will be essential to conclusively demonstrate that alterations in receptor composition are responsible for the increased run-down. Thus, further experiments, combining immunohistochemistry and single cell PCR for all major $GABA_A$ subunits with electrophysiology, will be needed to clarify the molecular and cellular mechanism of increased run-down.

Could the present observations be relevant in the human disease? In specimens obtained at surgery from TLE patients, signs of markedly impaired GABAergic transmission are evident. $GABA_A$ receptors, notably those containing α1 and α2 subunits, appear to redistribute within granule cells showing decreased expression in basal and increased expression in apical dendrites. Furthermore, substantial loss of α1-containg $GABA_A$ receptors has been observed in all parts of the Ammon's horn (2, 36). Data on α4 subunits are not yet available for the hippocampus of TLE patients.

In conclusion, the present data show: (*i*) that increased run-down occurs in the hippocampus at the time of the first spontaneous seizure and then extends to the cortex, remaining constant in the course of the disease; (*ii*) that this phenomenon is strictly correlated with the occurrence of spontaneous seizures (i.e., with the diagnosis of epilepsy), because it is never observed in resistant animals; (*iii*) suggest that alterations in $GABA_A$ receptor molecular composition within specific cell populations may be responsible for its development. These observations

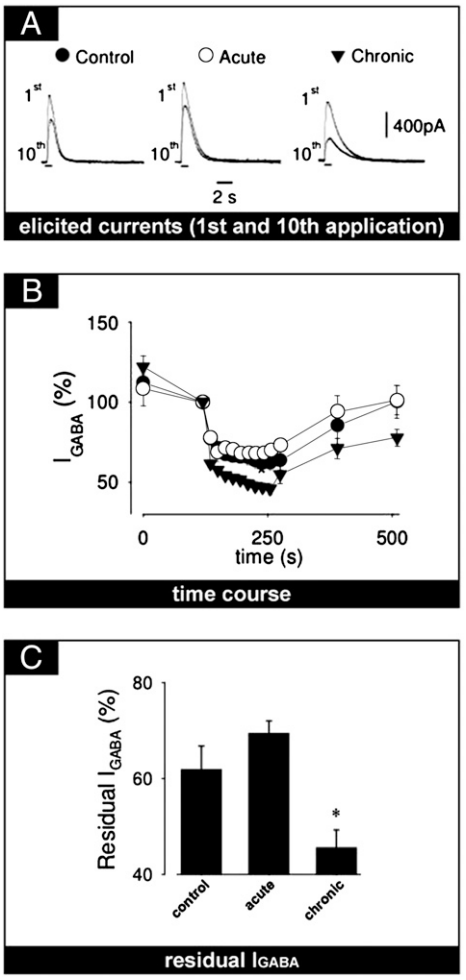

Fig. 4. Different I_{GABA} run-down upon repetitive stimulation in CA3 pyramidal neurons in hippocampal slices from control rats, pilocarpine-treated rats in acute phase (24 h after SE) and chronically epileptic rats. (*A*) Superimposed typical currents elicited by 1st and 10th GABA application (100 μM; 1-s duration every 15 s; horizontal bars; holding potential, 0 mV) during the repetitive stimulation protocol in CA3 hippocampal pyramidal neurons from control (*Left*), acutely pilocarpine-treated (*Center*) or chronic-epileptic rats (*Right*). (*B*) Time course of I_{GABA} averaged from 29 (●, control), 7 (○, acute) and 20 (▼, chronic) pyramidal neurons. Currents were normalized to the first I_{GABA} amplitude of the repetitive stimulation protocol. (*C*) Histogram of residual I_{GABA} (i.e., the ratio between tenth and first I_{GABA} amplitude) observed in CA3 pyramidal cells in the different conditions, as indicated. $*P <$ 0.02 vs. control and acute phase. ANOVA and post hoc Holm-Sidak test.

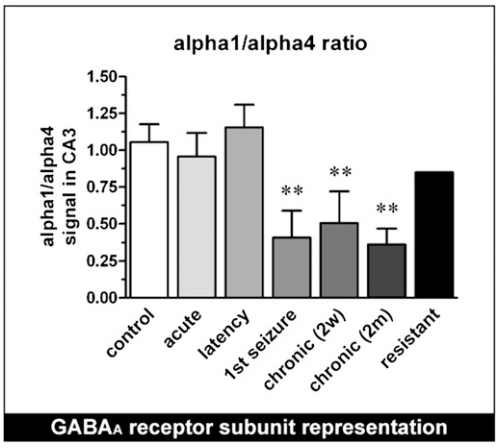

Fig. 5. Relative representation of the α1 and α4 subunits in CA3, at various time points after pilocarpine-induced SE. Note the appearance of a significant reduction in this ratio, expression of a relative increase in α4 subunits, at the time of the first spontaneous seizure. Similar results were obtained in the DG molecular layer. Data are the means ± SE of four to five animals per group. $**P < 0.05$ vs. control. ANOVA and post hoc Mann-Whitney *U* test.

disclose research opportunities that may lead to a better understanding of the mechanisms by which a previously normal tissue becomes epileptic. Importantly, this kind of research is technically feasible, amenable to verification in human tissue, and has the potential to lead to other therapies.

Materials and Methods

Animals. Male Sprague-Dawley rats (240–260 g; Harlan Italy) were used for all experiments. All procedures were carried out in accordance with European Community laws and policies.

Video-EEG. Video-EEG recordings were performed as previously described (18). See *SI Materials and Methods* for further information.

Tissue Preparation. At different times after injection of the chemoconvulsant, rats were killed and their brains were rapidly removed, immersed in 10% formalin and paraffin embedded. Coronal sections (6-μm thick) were cut across the dorsal hippocampus [160 sections, corresponding to 960 μm; plates 21– 23 of ref (37).].

Fluoro-Jade C Staining. FJC staining was performed as described (19). The quantification method was based on thresholding of digital images and calculation of the mean percent of FJC-positive pixels in the sections. Statistical analysis was conducted using the Mann-Whitney two-tailed *u* test (38). See *SI Materials and Methods* for further information.

Immunofluorescence. Immunofluorescence was performed as previously described (18). The primary antibodies were as follows: MAP2abc (mouse monoclonal, Immunological Sciences) and GFAP (rabbit polyclonal, Sigma) 1:25 and 1:50, respectively; NeuN (mouse monoclonal, Chemicon) 1:100; GFAP (as above) 1:50; MAP2abc (as above) and $GABA_A$ α1 receptor subunit [rabbit polyclonal (39, 40)] 1:25 and 1:50, respectively; parvalbumin (mouse monoclonal, Swant) and $GABA_A$ α1 receptor subunit (as above) both 1:50; GFAP (mouse monoclonal, Sigma) and $GABA_A$ α1 receptor subunit (as above) both 1:50; MAP2abc (as above) and $GABA_A$ α4 receptor subunit [rabbit polyclonal (39, 40)] 1:25 and 1:50, respectively; NeuN (as above) and $GABA_A$ α4 receptor subunit (as above) 1:100 and 1:50, respectively; GFAP (mouse monoclonal, Sigma) and $GABA_A$ α4 receptor subunit (as above) both 1:50. All antibodies were incubated overnight, except those for $GABA_A$ receptor subunits that were incubated for 3 days. The number of GFAP- and NeuN-positive cells was counted in 1,392 × 1,040 frames in various hippocampal subareas, as previously described (18). Statistical analysis was performed using ANOVA and post hoc Newman-Keuls test. See *SI Materials and Methods* for further information.

Immunohistochemistry. Immunohistochemistry was performed as previously described (18). Sections were incubated with the primary antibody for the $GABA_A$ α1 receptor subunit [rabbit polyclonal; 1:150 dilution (39, 40)] or for the α4 receptor subunit [rabbit polyclonal; 1:300 dilution (39, 40)]. Four regularly spaced sections have been examined per each subunit per animal. Images were transformed into gray levels, and the mean gray level was measured in the areas of interest. The numbers obtained in the four sections were averaged obtaining a single value per animal, and the value for α1 was divided by the one obtained for α4. Data were analyzed using the Mann-Whitney *U* test. See *SI Materials and Methods* for further information.

Membrane Preparation, Injection Procedures, and Electrophysiological Recordings from Oocytes. Rat tissue specimens were frozen in liquid nitrogen. Membranes were prepared as previously detailed (21). Preparation of *Xenopus laevis* oocytes and injection procedures were as detailed elsewhere (21). I_{GABA} run-down was defined as the decrease (in %) of the I_{GABA} peak amplitude at the sixth GABA jet (current-plateau) after five applications of GABA (1 mM, 10 s) at 40-s intervals. The fast I_{GABA} desensitization was measured as the time for 50% peak current decay ($T_{0.5}$). The holding

potential was −60 mV. I_{GABA} reversal potential was monitored at the first and sixth GABA applications by voltage ramps (from −100 to 30 mV, 1-s duration) during the current steady state, and control ramps were applied immediately before GABA applications. Data were analyzed using ANOVA. See *SI Materials and Methods* for further information.

Whole-Cell Recordings from Slices. Neocortical slices were prepared from adult rats (P36–P50) as described (9). Whole-cell patch-clamp recordings were performed on pyramidal neurons at 24–25 °C, as previously described (6), at a holding potential of 0 mV. The reduction in peak amplitude current was expressed as percent amplitude of current at the end of the run-down protocol vs. control ($I_{tenth}/I_{first} \times 100$). Data have been analyzed using ANOVA. For more details see ref. 5 and *SI Materials and Methods*.

ACKNOWLEDGMENTS. This paper is dedicated to the memory of Prof. Fabrizio Eusebi, our colleague and co-author. This work was supported by grants from the European Community [EU Research Grants LSH-CT-2006-037315 (EPICURE), thematic priority LIFESCIHEALTH to M.S., G.S., and P.F.F.], the Ministry of Health (to F.E. and E.P.), the Italian Ministry of Education and Research (Ministero dell'Istruzione, dell'Università e della Ricerca, MIUR-MIUR PRIN grant to E.P., M.S., and P.F.F.), the Mariani Foundation of Milan (Grant R-09-76 to F.E.), and the Fondazione Cariverona (to P.F.F.).

1. Pitkänen A, Sutula TP (2002) Is epilepsy a progressive disorder? Prospects for new therapeutic approaches in temporal-lobe epilepsy. *Lancet Neurol* 1:173–181.
2. Loup F, Wieser HG, Yonekawa Y, Aguzzi A, Fritschy JM (2000) Selective alterations in $GABA_A$ receptor subtypes in human temporal lobe epilepsy. *J Neurosci* 20:5401–5419.
3. Loup F, Picard F, Yonekawa Y, Wieser HG, Fritschy JM (2009) Selective changes in GABAA receptor subtypes in white matter neurons of patients with focal epilepsy. *Brain* 132:2449–2463.
4. Palma E, et al. (2005) Abnormal GABAA receptors from the human epileptic hippocampal subiculum microtransplanted to Xenopus oocytes. *Proc Natl Acad Sci USA* 102:2514–2518.
5. Ragozzino D, et al. (2005) Rundown of GABA type A receptors is a dysfunction associated with human drug-resistant mesial temporal lobe epilepsy. *Proc Natl Acad Sci USA* 102:15219–15223.
6. Palma E, et al. (2007) $GABA_{(A)}$-current rundown of temporal lobe epilepsy is associated with repetitive activation of $GABA_{(A)}$ "phasic" receptors. *Proc Natl Acad Sci USA* 104:20944–20948.
7. Palma E, et al. (2004) Phosphatase inhibitors remove the run-down of gamma-aminobutyric acid type A receptors in the human epileptic brain. *Proc Natl Acad Sci USA* 101:10183–10188.
8. Palma E, et al. (2005) BDNF modulates $GABA_A$ receptors microtransplanted from the human epileptic brain to Xenopus oocytes. *Proc Natl Acad Sci USA* 102:1667–1672.
9. Roseti C, et al. (2008) Adenosine receptor antagonists alter the stability of human epileptic GABAA receptors. *Proc Natl Acad Sci USA* 105:15118–15123.
10. Roseti C, et al. (2009) Blockage of A2A and A3 adenosine receptors decreases the desensitization of human GABA(A) receptors microtransplanted to Xenopus oocytes. *Proc Natl Acad Sci USA* 106:15927–15931.
11. Laschet JJ, et al. (2007) Dysfunction of $GABA_A$ receptor glycolysis-dependent modulation in human partial epilepsy. *Proc Natl Acad Sci USA* 104:3472–3477.
12. Fabene PF, et al. (2008) A role for leukocyte-endothelial adhesion mechanisms in epilepsy. *Nat Med* 14:1377–1383.
13. Vezzani A (2009) Pilocarpine-induced seizures revisited: What does the model mimic? *Epilepsy Curr* 9:146–148.
14. Pitkanen A, Schwartzkroin PA, Moshè SL (2006) *Models of seizures and epilepsy* (Elsevier Academic Press, Burlington, MA).
15. Racine RJ (1972) Modification of seizure activity by electrical stimulation. II. Motor seizure. *Electroencephalogr Clin Neurophysiol* 32:281–294.
16. Goffin K, Nissinen J, Van Laere K, Pitkänen A (2007) Cyclicity of spontaneous recurrent seizures in pilocarpine model of temporal lobe epilepsy in rat. *Exp Neurol* 205: 501–505.
17. Curia G, Longo D, Biagini G, Jones RS, Avoli M (2008) The pilocarpine model of temporal lobe epilepsy. *J Neurosci Methods* 172:143–157.
18. Paradiso B, et al. (2009) Localized delivery of fibroblast growth factor-2 and brain-derived neurotrophic factor reduces spontaneous seizures in an epilepsy model. *Proc Natl Acad Sci USA* 106:7191–7196.
19. Schmued LC, Stowers CC, Scallet AC, Xu L (2005) Fluoro-Jade C results in ultra high resolution and contrast labeling of degenerating neurons. *Brain Res* 1035:24–31.
20. Garzillo CL, Mello LE (2002) Characterization of reactive astrocytes in the chronic phase of the pilocarpine model of epilepsy. *Epilepsia* 43 (Suppl 5):107–109.
21. Miledi R, Palma E, Eusebi F (2006) Microtransplantation of neurotransmitter receptors from cells to Xenopus oocyte membranes: New procedure for ion channel studies. *Methods Mol Biol* 322:347–355.
22. Eusebi F, Palma E, Amici M, Miledi R (2009) Microtransplantation of ligand-gated receptor-channels from fresh or frozen nervous tissue into Xenopus oocytes: A potent tool for expanding functional information. *Prog Neurobiol* 88:32–40.
23. Palma E, et al. (2003) Microtransplantation of membranes from cultured cells to Xenopus oocytes: A method to study neurotransmitter receptors embedded in native lipids. *Proc Natl Acad Sci USA* 100:2896–2900.
24. Brooks-Kayal AR, Shumate MD, Jin H, Rikhter TY, Coulter DA (1998) Selective changes in single cell GABA(A) receptor subunit expression and function in temporal lobe epilepsy. *Nat Med* 4:1166–1172.
25. Peng Z, Houser CR (2005) Temporal patterns of fos expression in the dentate gyrus after spontaneous seizures in a mouse model of temporal lobe epilepsy. *J Neurosci* 25: 7210–7220.
26. Sperk G, Furtinger S, Schwarzer C, Pirker S (2004) *Recent Advances in Epilepsy Research*, eds Binder DK, Scharfman HE (Kluwer Academic/Plenum Publishers, New York, NY), pp 92–103.
27. Sperk G (2007) Changes in $GABA_A$ receptors in status epilepticus. *Epilepsia* 48 (Suppl 8):11–13.
28. Zhang G, Raol YH, Hsu FC, Coulter DA, Brooks-Kayal AR (2004) Effects of status epilepticus on hippocampal GABAA receptors are age-dependent. *Neuroscience* 125: 299–303.
29. Poulter MO, et al. (1999) Differential expression of α1, α2, α3, and α5 $GABA_A$ receptor subunits in seizure-prone and seizure-resistant rat models of temporal lobe epilepsy. *J Neurosci* 19:4654–4661.
30. Raol YH, et al. (2006) Enhancing $GABA_{(A)}$ receptor alpha 1 subunit levels in hippocampal dentate gyrus inhibits epilepsy development in an animal model of temporal lobe epilepsy. *J Neurosci* 26:11342–11346.
31. Lagrange AH, Botzolakis EJ, Macdonald RL (2007) Enhanced macroscopic desensitization shapes the response of alpha4 subtype-containing $GABA_A$ receptors to synaptic and extrasynaptic GABA. *J Physiol* 578:655–676.
32. Sperk G, Wieselthaler-Hoelzl A, Drexel M (2009) *Encyclopedia of Basic Epilepsy Research*, ed Schwartzkroin P (Elsevier/Academic Press, Amsterdam), pp 10351–10356.
33. Schwarzer C, et al. (1997) $GABA_{(A)}$ receptor subunits in the rat hippocampus II: Altered distribution in kainic acid-induced temporal lobe epilepsy. *Neuroscience* 80: 1001–1017.
34. Nishimura T, et al. (2005) Altered expression of GABA(A) and GABA(B) receptor subunit mRNAs in the hippocampus after kindling and electrically induced status epilepticus. *Neuroscience* 134:691–704.
35. Zhang N, Wei W, Mody I, Houser CR (2007) Altered localization of GABA(A) receptor subunits on dentate granule cell dendrites influences tonic and phasic inhibition in a mouse model of epilepsy. *J Neurosci* 27:7520–7531.
36. Pirker S, et al. (2003) Increased expression of $GABA_{(A)}$ receptor beta-subunits in the hippocampus of patients with temporal lobe epilepsy. *J Neuropathol Exp Neurol* 62: 820–834.
37. Paxinos G, Watson C (1982) *The Rat Brain in Stereotaxic Coordinates* (Academic Press, New York, USA).
38. Zucchini S, et al. (2008) Fgf-2 overexpression increases excitability and seizure susceptibility but decreases seizure-induced cell loss. *J Neurosci* 28:13112–13124.
39. Sperk G, Schwarzer C, Tsunashima K, Fuchs K, Sieghart W (1997) $GABA_{(A)}$ receptor subunits in the rat hippocampus I: Immunocytochemical distribution of 13 subunits. *Neuroscience* 80:987–1000.
40. Pirker S, Schwarzer C, Wieselthaler A, Sieghart W, Sperk G (2000) $GABA_{(A)}$ receptors: Immunocytochemical distribution of 13 subunits in the adult rat brain. *Neuroscience* 101:815–850.

Supporting Information

Mazzuferi et al. 10.1073/pnas.0914710107

SI Materials and Methods

Animals. Male Sprague-Dawley rats (240–260 g; Harlan Italy) were used for all experiments. Animals were housed under standard conditions: constant temperature (22–24 °C) and humidity (55–65%), 12-h dark-light cycle, and free access to food and water. All efforts were made to minimize animal suffering. Procedures involving animals and their care were carried out in accordance with European Community and national laws and policies.

Pilocarpine. Pilocarpine was administered i.p. (300 mg/kg), and behavior was observed for several hours thereafter. Within the first hour after injection, all animals developed seizures evolving into recurrent generalized convulsions (SE). SE was interrupted 3 h after onset by administration of diazepam (10 mg/kg i.p.).

One week before pilocarpine administration, a radiotelemetry transmitter (Data Sciences International, DSI PhysioTel Transmitters) was surgically implanted for EEG diagnostic. Rats were anesthetized with 1 mL/kg medetomidine and zolazepam/tiletamine. An incision was made in the linea alba, the body of the transmitter was placed in the abdominal cavity, and the incision was then sutured attaching the body of the transmitter to the inner surface of the abdominal cavity. Two catheters containing electrodes were led subcutaneusly from the abdomen to an incision made under the skull, crossing the animal's body near the shoulder blade. Electrodes were inserted in the cortical zone and fixed with blue glue and dental cement. After surgery, rats were administered a prophylactic antibiotic therapy (amoxycillin and clavulanic acid) and a peripherally acting analgesic agent (carprofen), and allowed a week of recovery.

Seizure onset, severity, and duration were assessed by 24/24-h video-EEG monitoring of the animals, performed by means of Phenotyper cages (Noldus Information Technology) and an EEG acquisition system using telemetric technology (Dataquest A.R.T. Data Acquisition 3.0 for telemetry systems, Data Sciences International). Behavioral seizures were scored according to the scale of Racine (1). Visual scoring was performed by two independent researchers. Seizure detection (duration and severity), as well as single ictal events (2 s), were scored for each individual rat for the whole analysis period.

Tissue Preparation. Rats were killed at different time points after injection of the chemoconvulsant (as described above) by decapitation after an anesthetic overdose. Their brains were rapidly removed, immersed in 10% formalin, and then paraffin embedded. Coronal sections (6 μm thick) were cut across the dorsal hippocampus (plates 21–23 of ref. 2) and mounted onto polarized slides (Superfrost slides, Diapath). To standardize the cutting level, one section of every 10 was used for hematoxylin-eosin staining: sections were dewaxed (two washes in xylol for 10 min, 5 min in ethanol 100%, 5 min in ethanol 95%, 5 min in ethanol 80%), incubated in Mayer's hematoxylin solution (5 min), washed in water (5 min), incubated in alcohol eosin solution (2 min), and dehydrated; coverslips were mounted using DPX Mountant for histology (Fluka BioChemika).

Fluoro-Jade C Staining. FJC staining was performed as described by Schmued et al. (3). Briefly, sections were dewaxed as described above and incubated in a solution containing 1% NaOH in 80% ethanol (5 min), then in 70% ethanol (2 min), then in distilled water (2 min). Subsequently, they were incubated for 10 min in 0.06% potassium permanganate, washed for 2 min in distilled water, and transferred to a 0.001% FJC staining solution. After staining, sections were washed three times in distilled water. The slices were then dried for 30 min at 50 °C.

FJC analysis was conducted using a Leica microscope (DMRA2; Leica Italia). The quantification method was based on the thresholding of FJC digital images (4). Images of the hippocampus were captured using a Leica DFC300FX camera and transformed into gray levels. Using Photoshop CS2 (version 9.0.2), the hippocampus was cut out and the mean ± SD gray level was calculated. FJC-positive pixels were identified by thresholding at the gray level corresponding to the mean plus three standard deviations. Using this approach, only those pixels that were significantly above background (that is, positive to FJC) were selected. Data were then expressed as percent of FJC-positive pixels over total cortical or hippocampal pixels. The mean percent of FJC-positive pixels in the sections examined was calculated for each animal and used for statistical analysis. Statistical analysis was conducted using the Mann-Whitney two-tailed U test.

Immunofluorescence. Sections were dewaxed and rehydratated as described above. All antigens were unmasked using a commercially available kit (Unmasker, Diapath), according to the manufacturer's instructions. After washing in PBS, sections were incubated with Triton x-100 (0.3% in PBS 1×, room temperature, 10 min), washed twice in PBS 1×, and incubated with 5% BSA and 5% serum of the species in which the secondary antibody was produced for 30 min. They were then incubated in humid atmosphere with the primary antibodies at 4 °C, as follows: MAP2abc (mouse monoclonal, Immunological Sciences) and GFAP (rabbit polyclonal, Sigma) 1:25 and 1:50, respectively; NeuN (mouse monoclonal, Chemicon) 1:100; GFAP (as above) 1:50; MAP2abc (as above) and $GABA_A$ α1 receptor subunit (rabbit polyclonal; 5, 6) 1:25 and 1:50, respectively; parvalbumin (mouse monoclonal, Swant) and $GABA_A$ α1 receptor subunit (as above) both 1:50; GFAP (mouse monoclonal, Sigma) and $GABA_A$ α1 receptor subunit (as above) both 1:50; MAP2abc (as above) and $GABA_A$ α4 receptor subunit (rabbit polyclonal; 5, 6) 1:25 and 1:50, respectively; NeuN (as above) and $GABA_A$ α4 receptor subunit (as above) 1:100 and 1:50, respectively; GFAP (mouse monoclonal, Sigma) and $GABA_A$ α4 receptor subunit (as above) both 1:50. All antibodies were incubated overnight, except those for $GABA_A$ receptor subunits that were incubated for three days. After 5-min rinses in PBS, sections were exposed again to Triton (30 min), washed in PBS, and incubated with the goat antimouse Alexa Fluor 488-conjugated, secondary antibody (1:500 dilution; Invitrogen) for mouse primary antibodies, or with a goat antirabbit, Alexa Fluor 594-conjugated, secondary antibody (1:500; Invitrogen) for rabbit primary antibodies, at room temperature for 3 h. After staining, sections were washed in PBS, counterstained with 0.0001% DAPI for 10 min, and washed again. Coverslips were mounted using anti fading Gel/Mount water based (Biomeda).

The number of GFAP- and NeuN-positive cells was counted in 1,392 × 1,040 frames in various hippocampal subareas, as previously described (7). Images were acquired through a Leica DFC300 FX video camera mounted on a Leica DMRA2 microscope and analyzed in a blinded manner by two investigators, using the program Leica FW 4000. Images were captured with a 20× objective. Data obtained from the multiple sections examined for each rat were averaged to obtain a single estimate for

each animal. Statistical analysis was performed using ANOVA and post hoc Newman-Keuls test.

Immunohistochemistry. Sections were dewaxed, rehydratated, and unmasked as described above and then washed in PBS 1× for 10 min. After incubation in H_2O_2 0.3% for 15 min at room temperature, sections were rapidly rinsed in distilled water and washed twice in PBS for 5 min each. They were then incubated with Ultra V Block (Thermo Scientific), washed again in PBS 1×, and incubated for 3 days at 4 °C in humid atmosphere with the primary antibody for the $GABA_A$ α1 receptor subunit (rabbit polyclonal; 1:150 dilution; 5, 6) or for the α4 receptor subunit (rabbit polyclonal; 1:300 dilution; 5, 6). Incubation with biotynilated goat antipolyvalent serum and with streptavidin peroxidase was conducted according to the manufacturer's instructions (LabVision Corporation). The reaction product was detected as a brown substrate using DAB (Vector Laboratories). Finally, sections were washed three times (once in distillate water and twice in PBS 1×), 5 min each. Coverslips were mounted using Shur/Mount (TBS). The specificity of immunolabeling was verified in all experiments by controls in which the primary antibody was omitted.

As stated above, paraffin-embedded brains were cut in successive 6-μm sections across the entire dorsal hippocampus [i.e., 160 sections, corresponding to 960 μm; plates 21–23 of ref. 2]. One every 40 of these sections was stained for α1 and α4, as described above. Thus, four regularly spaced sections have been examined per each subunit per animal. Images were captured using a Leica DFC300FX camera mounted on a Leica microscope (DMRA2, Leica). Illumination was kept constant throughout all experiments. Using Photoshop CS2 (version 9.0.2), images were transformed in gray levels, the areas of interest (DG, CA3, CA1, and the different layers in each) were cut out, and the mean gray level was calculated. The gray level in the callosum was subtracted to obtain the net signal. An estimate of the signal in the area under examination across the dorsal hippocampus was obtained by averaging the numbers obtained in the five examined sections, obtaining a single value per animal that was used for statistical analysis. Finally, the signal produced by α1 was divided by the one produced by α4. The data obtained were analyzed using the Mann-Whitney *U* test.

Membrane Preparation, Injection Procedures, and Electrophysiological Recordings from Oocytes. Rat tissue specimens were frozen in liquid nitrogen immediately after dissection. Membranes were prepared as previously detailed (8). Preparation of *X. laevis* oocytes and injection procedures were as detailed elsewhere (8). From 12 to 48 h after injection, membrane currents were recorded from voltage-clamped oocytes using two microelectrodes filled with 3 M KCl. The oocytes were placed in a recording chamber (volume, 0.1 mL) perfused continuously (9-10 mL/min) with oocyte Ringer at room temperature (20-22 °C). I_{GABA} run-down was defined as the decrease (in percentage) of the I_{GABA} peak amplitude at the sixth GABA jet (current-plateau) after five applications of GABA (1 mM), 10-s duration, at 40-s intervals. The fast I_{GABA} desensitization was measured as the time for 50% peak current decay ($T_{0.5}$). In all experiments the holding potential was −60 mV. Data have been analyzed using ANOVA.

Whole-Cell Recordings from Slices. Neocortical slices were prepared from adult rats (P36-P50) as described (9). Transverse slices (250 μm) were cut in glycerol-based artificial cerebro-spinal fluid (ACSF) with a vibratome (Leica VT 1000S; Leica Microsystems); placed in a slice incubation chamber at room temperature with oxygenated ACSF and transferred to a recording chamber within 1–12 h after slice preparation. Whole-cell patch clamp recordings were performed on pyramidal neurons at 24–25 °C, as previously described (10), at a holding potential of 0 mV. Membrane currents were recorded using glass electrodes (3-4 MΩ) filled with (in mM): 140 K-gluconate, 10 hepes, 5 BAPTA, 2 Mg-ATP (pH 7.3, with KOH). GABA was delivered to cells by pressure applications (10-20 psi; 1 s; Picospritzer II, General Valve) from glass micropipettes positioned above whole-cell voltage-clamped neurons. In this way, we obtained stable whole-cell currents and rapid drug wash before applying the run-down protocol. The current run-down protocol adopted was the following: after current amplitude stabilization with repetitive applications every 120 s, a sequence of 10 GABA (100 μM) applications every 15 s was delivered; the test pulse was resumed at control rate (every 120 s) to monitor recovery of I_{GABA}. The reduction in peak amplitude current was expressed as percentage amplitude of current at the end of the run-down protocol vs. control ($I_{tenth}/I_{first} \times 100$). Data have been analyzed using ANOVA. For more details see ref. 11.

Chemicals and Solutions. Oocyte Ringer had the following composition (in mM): NaCl 82.5; KCl 2.5; $CaCl_2$ 2.5; $MgCl_2$ 1; Hepes 5, adjusted to pH 7.4 with NaOH. ACSF had the following composition (in mM): 125 NaCl, 2.5 KCl, 2 $CaCl_2$, 1.25 NaH_2PO_4, 1 $MgCl_2$, 26 $NaHCO_3$, 10 glucose (pH 7.35). Glycerol-based ACSF solution contained (mM): glycerol 250; KCl 2.5; $CaCl_2$ 2.4; $MgCl_2$ 1.2; NaH_2PO_4 1.2; $NaHCO_3$ 26; glucose 11; Na-pyruvate 0.1 (pH 7.35). All drugs were purchased from Sigma with the exception of GABA that was purchased from Tocris.

1. Racine RJ (1972) Modification of seizure activity by electrical stimulation. II. Motor seizure. *Electroencephalogr Clin Neurophysiol* 32:281–294.
2. Paxinos G, Watson C (1982) *The Rat Brain in Stereotaxic Coordinates* (Academic Press, New York, USA).
3. Schmued LC, Stowers CC, Scallet AC, Xu L (2005) Fluoro-Jade C results in ultra high resolution and contrast labeling of degenerating neurons. *Brain Res* 1035: 24–31.
4. Zucchini S, *et al.* (2008) Fgf-2 overexpression increases excitability and seizure susceptibility but decreases seizure-induced cell loss. *J Neurosci* 28:13112–13124.
5. Pirker S, Schwarzer C, Wieselthaler A, Sieghart W, Sperk G (2000) $GABA_A$ receptors: Immunocytochemical distribution of 13 subunits in the adult rat brain. *Neuroscience* 101:815–850.
6. Sperk G, Schwarzer C, Tsunashima K, Fuchs K, Sieghart W (1997) $GABA_A$ receptor subunits in the rat hippocampus I: Immunocytochemical distribution of 13 subunits. *Neuroscience* 80:987–1000.
7. Paradiso B, *et al.* (2009) Localized delivery of fibroblast growth factor-2 and brain-derived neurotrophic factor reduces spontaneous seizures in an epilepsy model. *Proc Natl Acad Sci USA* 106:7191–7196.
8. Miledi R, Palma E, Eusebi F (2006) Microtransplantation of neurotransmitter receptors from cells to Xenopus oocyte membranes: New procedure for ion channel studies. *Methods Mol Biol* 322:347–355.
9. Gabriel S, *et al.* (2004) Stimulus and potassium-induced epileptiform activity in the human dentate gyrus from patients with and without hippocampal sclerosis. *J Neurosci* 24:10416–10430.
10. Palma E, *et al.* (2007) $GABA_A$-current rundown of temporal lobe epilepsy is associated with repetitive activation of $GABA_A$) "phasic" receptors. *Proc Natl Acad Sci USA* 104:20944–20948.
11. Ragozzino D, *et al.* (2005) Rundown of GABA type A receptors is a dysfunction associated with human drug-resistant mesial temporal lobe epilepsy. *Proc Natl Acad Sci USA* 102:15219–15223.

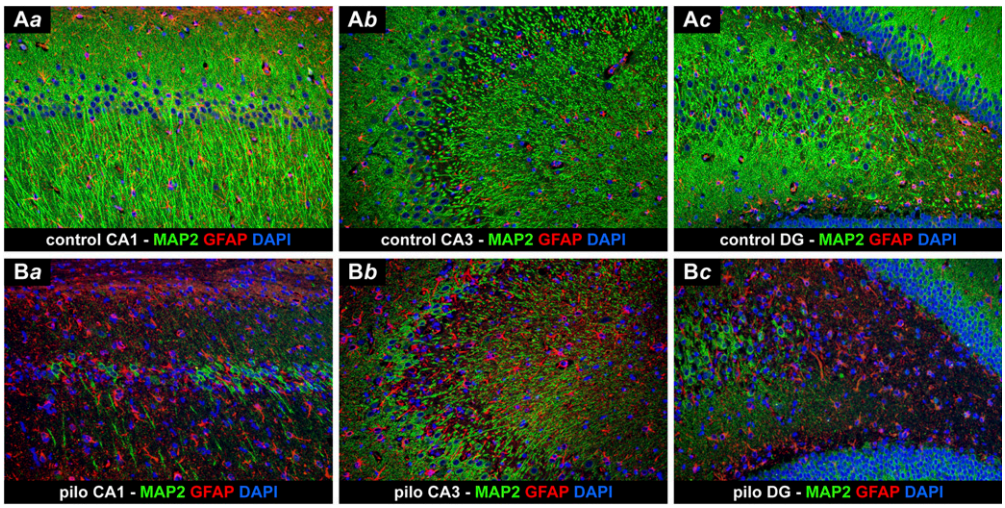

Fig. S1. Neuropathological outcome during latency, 5 days after pilocarpine-induced SE. Sections taken across the dorsal hippocampus of control (*A*) and pilocarpine (pilo) rats (*B*) killed 5 days after SE. Neurons (MAP2-positive) in green, astrocytes (GFAP-positive) in red, nuclei (DAPI-positive) in blue. Note the dramatic astrocytosis and neuronal loss in the pilocarpine rats CA1 (*Ba*), CA3 (*Bb*) and dentate gyrus (*Bc*).

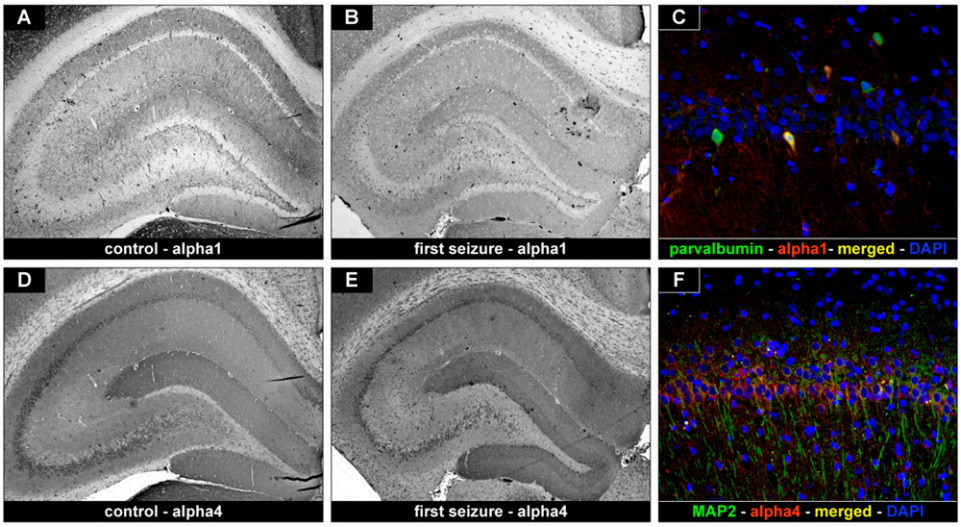

Fig. S2. Representation of α1 (*A*–*C*) and α4 (*D* and *E*) receptor subunits in the hippocampus of control animals (*A* and *D*) and at the time of the first spontaneous seizure (*B* and *E*). (*C*) Prevalent localization of the α1 subunit in parvalbumin-positive interneurons. Parvalbumin in green, α1 subunit in red, nuclei (DAPI-positive) in blue, parvalbumin and α1 subunit colocalization in yellow. (*F*) Prevalent localization of the α4 subunit in principal neurons. Neurons (MAP2-positive) in green, α4 subunit in red, nuclei (DAPI-positive) in blue, MAP2 and α4 subunit colocalization in yellow. Similar results were obtained using NeuN instead of MAP2 to label neurons.

Table S1. Run-down of I_{GABA} in oocytes microtransplanted with membranes from epileptic rats at different time points in the course of the disease

Rats (tested animals)	I_{GABA}, %	
	Hippocampus, *n*/frogs	Cortex, *n*/frogs
Control (4)	68 ± 6 (32/3)	70 ± 4 (56/6)
Acute (4)	63 ± 3 (30/3)	68 ± 4 (30/3)
Latency (4)	64 ± 4 (25/3)	71 ± 5 (30/4)
First seizure (5)	28 ± 6 (60/5)	65 ± 3 (65/6)
Chronic 2 weeks (3)	31 ± 3 (66/6)	35 ± 4 (70/8)
Chronic 2 months (2)	24 ± 1 (25/3)	37 ± 4 (30/3)
Resistant (3)	60 ± 2 (35/4)	64 ± 3 (35/4)

n = number of oocytes tested. I_{GABA} (%) values represent the sixth I_{GABA} amplitude normalized to the first one of the run-down protocol. Data are the means ± SEM of 25–70 oocytes per group (two to five rats, three to eight frogs).